Studies of TTF RF Photocathode Gun using acoustic sensors

J. Nelson and M. Ross
SLAC
November 27, 2001

Abstract:

The arc that occurs during RF breakdown is known to cause local heating of a copper cavity surface, with temperatures sometimes exceeding the melting point. Thermally generated acoustic shock waves [1,2] that accompany breakdowns can be easily detected on the surface of the cavity using externally mounted sensors. Acoustic emission sensors [3] have been used at the TESLA Test Facility to find RF high voltage breakdown locations in the photocathode gun system. It is not known if the acoustic signal emitted from the source (cathode) of the arc is stronger than that emitted from its terminus. The start time and root mean square amplitude of the signal from each of several sensors can be used to locate and classify the breakdown event. We report here on the use of eight sensors mounted on the TTF RF gun [4] to locate its breakdown events during operation with a pulse length of 300μs and a pulse amplitude up to 35 MeV/m.

Introduction:

Acoustic emission is used in a variety of accelerator and industrial non-destructive testing applications, a notable example being crack propagation in airplane frames. The acoustic signal emitted from a copper structure following a breakdown event is very large compared to that associated with crack propagation and has a characteristic frequency near 300 KHz. It is easily heard inside the accelerator enclosure in spite of its high frequency. Three kinds of acoustic waves of propagate in copper, bulk shear waves with a speed v_s = 2.325 mm/μs, bulk pressure waves, v_b = 4.760 mm/μs, and a slower surface shear wave (probably not of interest here). The shear wave disturbance wavelength is about 10 mm, small compared to the dimensions of the gun assembly.

Acoustic emission sensors are basically small, high frequency microphones [5] made of a small disk of piezo-electric material. Even though the relative sensor amplitude response calibration varies up to a factor of 2, the start times, t_0, are an accurate representation of the arrival of the wave. The sensors are not calibrated in an absolute sense, i.e. we do not have an estimate for the amplitude or direction of the mechanical motion. They are readily glued to the outside of the cavity. A nearby amplifier is needed to boost the signal so it can be recorded in a waveform recorder located outside the beamline enclosure.

Installation and use at the TTF:

Eight sensors were attached to the TTF RF gun in three different configurations, one of which is shown in figure 1. In order to search for breakdowns in three sections of the gun, the sensors were placed 1) along the side of the rectangular waveguide as it approaches the coupler cell, 2) around the waveguide directly above the coupler cell iris and 3)

around the 1.5 cell structure itself. The sensors were attached to the clean copper surface using cyano-acrylate very quick setting glue. Each sensor is connected to a SLAC-built variable gain AC coupled amplifier which has about 10 MHz bandwidth. The amplifier [6] is connected to oscilloscopes located outside of the beam enclosure. For most of the data, the oscilloscope was triggered by the fast reflected energy detector interlock used to protect the gun. The interlock is connected to the reflected energy (RE) port of the directional coupler near the end of the rectangular waveguide. The trigger is used to rapidly remove the drive from the klystron (klystron 3), during the pulse, so that the energy delivered to the breakdown is minimum. It should be synchronized to the breakdown.

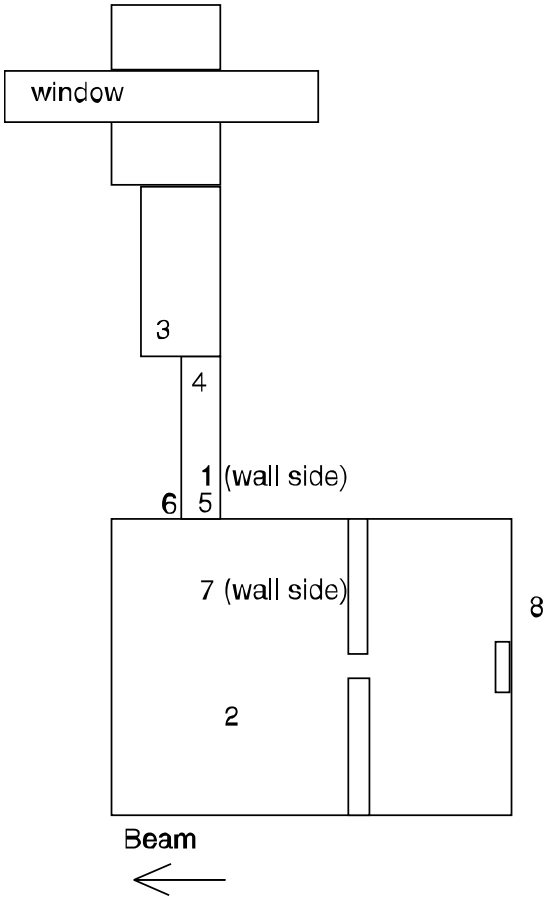

Figure 1: Elevation outline of the TTF RF gun assembly showing the locations of the acoustic sensors for configuration 2. The beam is emitted from the cathode at the right side of the sketch and the RF from the klystron comes through the waveguide from the top of the sketch.

The sensor locations are indicated by the numerals in figure 1. Four were fixed to the L band waveguide and 4 to the body of the gun. For analysis, these were divided into 3 groups, the three on the L-band rectangular waveguide (5, 4 and 3) those around the coupler iris (6, 5, and 1) and the four around the gun body (6, 7, 2 and 8). Of the 8 sensors, number 6 is mounted closest to the coupling iris and number 8 is nearest the cathode.

For each of the breakdown events, all 8 scope traces, 0.5 ms in length, were read into the computer using the MATLAB/GPIB interface. Figure 2 shows a typical set of scope traces with the strong oscillatory behavior characteristic of acoustic motion. Without breakdown, the sensor signal is about 7 mV rms, and is barely distinguishable from the noise signal present without RF. The traces in figures 2 and 3 clearly show differences in their amplitude envelope and t_0. In some, a clear prompt pulse at about 100μs is seen. Based on tests done with a sensor suspended in the air near the waveguide, we believe the prompt pulse is caused by radiation either in the sensor or nearby amplifier.

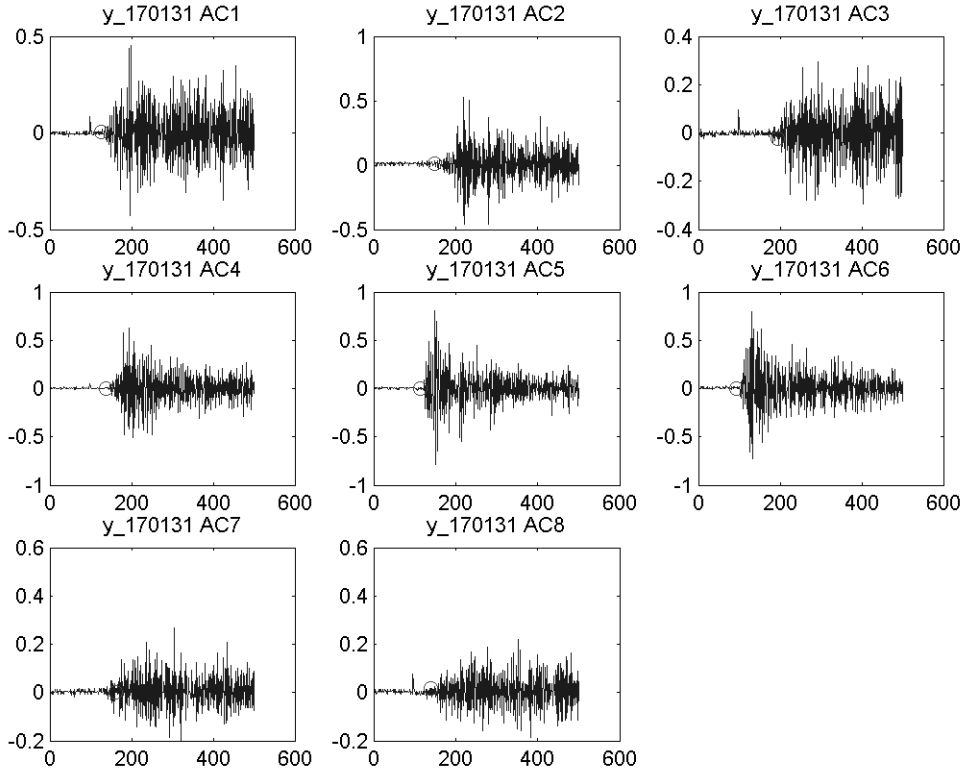

Figure 2: Recorded voltage signals from TTF gun acoustic sensors. The horizontal scale is in microseconds and the vertical scale is in volts.

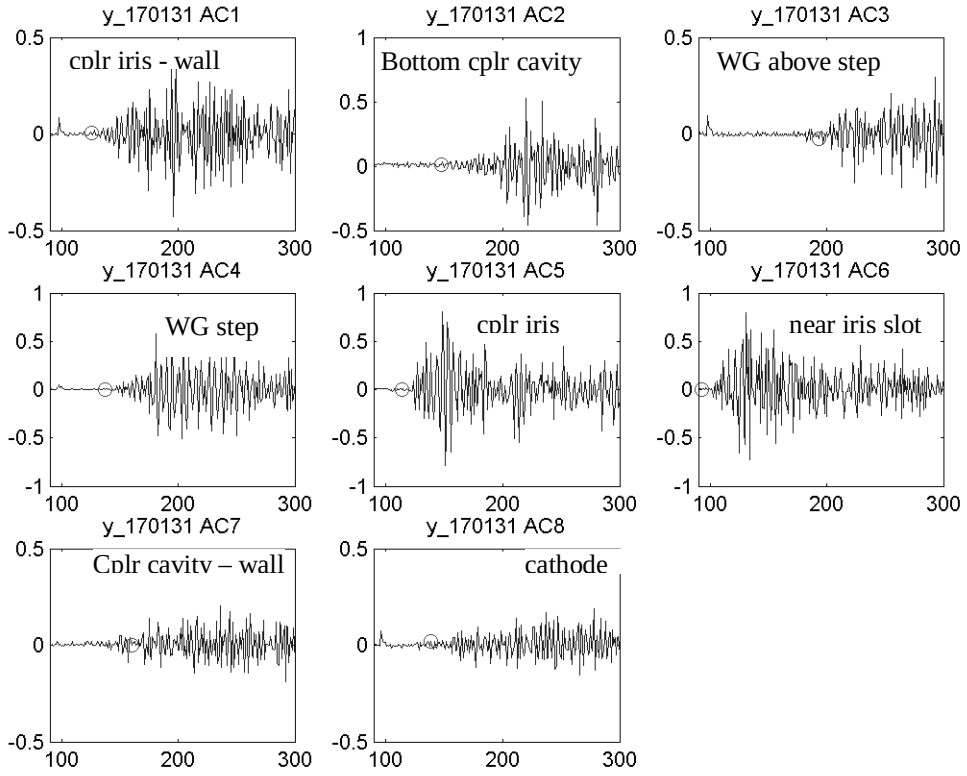

Figure 3: Close up view of the signals shown in figure 2. The circles indicate the estimated t_0. The title for each small plot shows the time the data was recorded and the amplifier channel (AC#, see table 1 below). The horizontal scale is in microseconds.

Data and Analysis:

The source of the acoustic signal is presumably at either end of an 'arc' or strong electron current flow. Signals from 56 breakdown events with 2 different sensor configurations were recorded. Of the 56, data from 41 are shown in figures 4-8 below. The 15 excluded traces were either poorly triggered or background events. In order to estimate the moment at which the sensor first responded to the breakdown event, a start time, t_0, was determined for each trace. For the purpose of trying to locate the source of the acoustic disturbance, the sensors are divided into the 3 groups indicated above. Since the earliest acoustic signal, coming from the sensor closest to the breakdown, is associated with the sensors nearest the power input coupling iris, we tabulated the path lengths from sensor 5 (see Figure 1) to each of the other sensors. Table 1 shows the distances for configuration 2.

Table 1: Path length from sensor 5 to each of the other sensors. See figure 1.

Sensor number (amplifier channel)	Associated group of sensors	Distance from sensor # 5 (mm)
1	Coupler iris (wall side)	273
2	Lower part of cavity coupler cell	186
3	Rectangular waveguide – above step	187
4	Rectangular waveguide	95
5	Coupler iris (aisle side)	0 (datum)
6	Coupler iris (near internal slot)	75
7	Cavity coupler cell – wall side	356
8	Cavity (cathode)	150

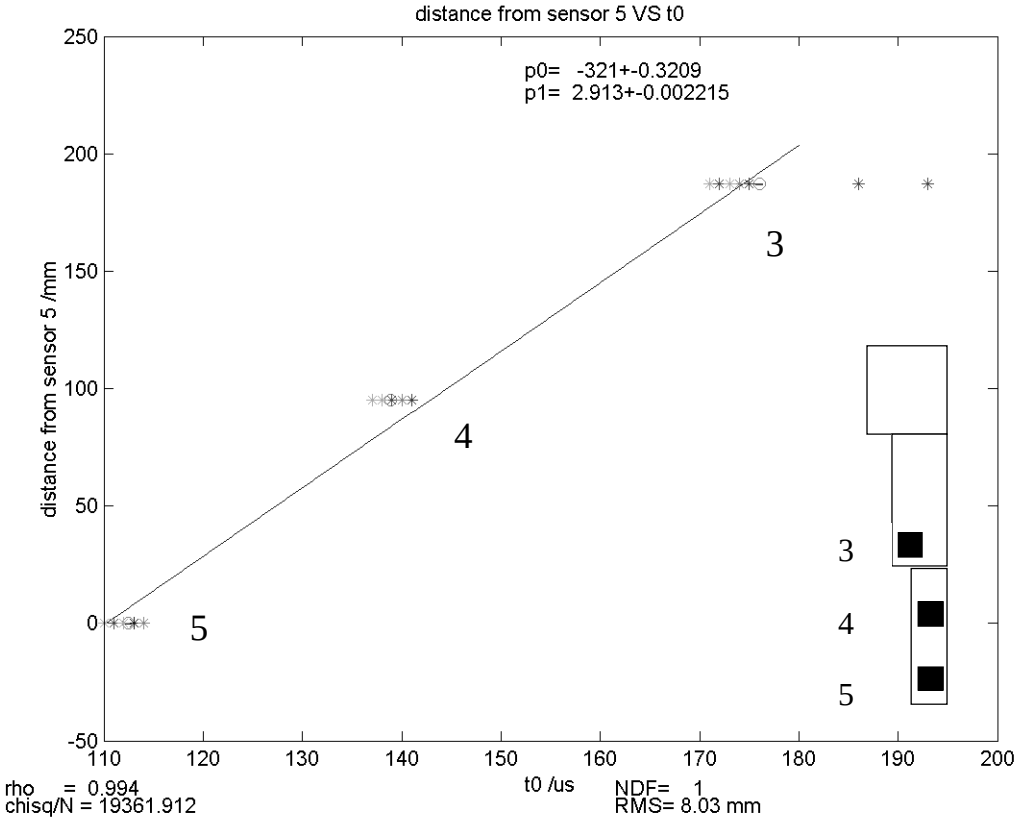

Figure 4: Sensor distance (numbers 5, 4 and 3) from sensor 5 vs the estimated start times of oscillation in the scope trace, t_0, for configuration B (16 breakdown events). The '*' marks t_0 for each trace and the 'o' marks the mean t_0 for the 16 traces. The numerals indicate the sensor number with the side view of the waveguide in the lower right corner of the plot showing approximate sensor locations.

Figure 4 shows t_0 for the three L-band waveguide sensors (#5, 4, and 3). Since the earliest sensor to respond is at the bottom of the waveguide and the sensors above that one respond in succession, it is reasonable to assume that an acoustic disturbance emerges from near the bottom of the waveguide. The data fall on a line with a fit slope (p1) v = 2.9 mm/μs, a value between v_s and v_b.

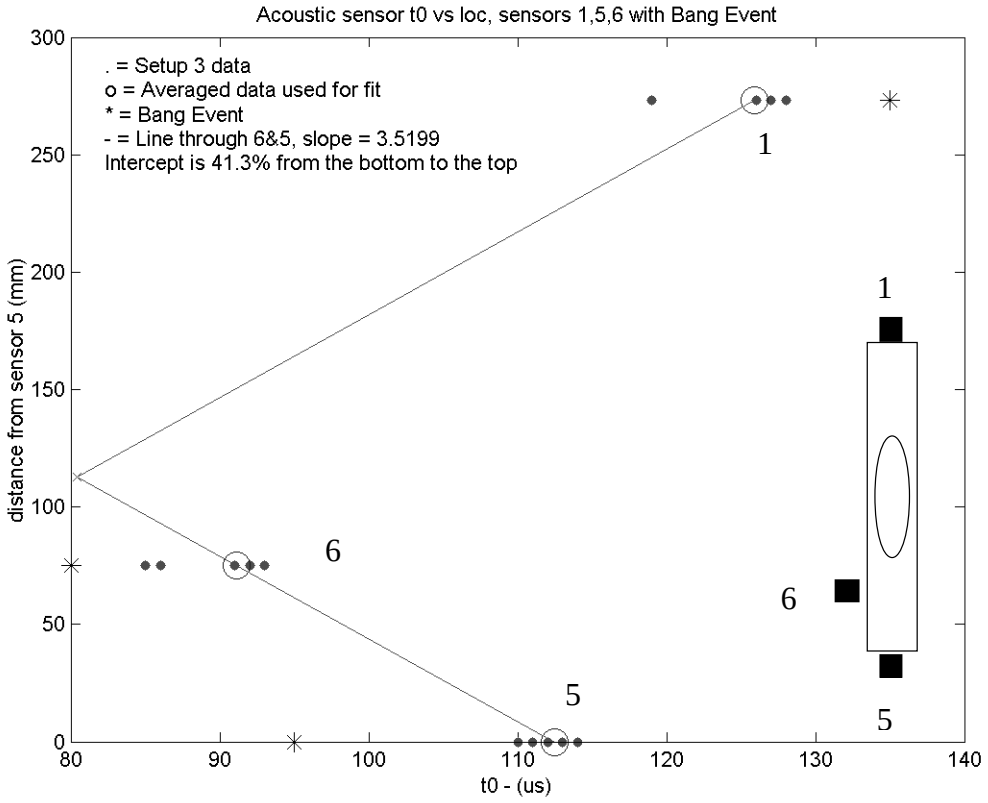

Figure 5: Sensor distance from sensor 5 vs t_0 for the sensors mounted around the periphery of the rectangular waveguide at its connection point to the coupler cavity. The numerals indicate the sensor number with a top view of the waveguide, looking down from above, in the lower right hand corner of the figure showing approximate sensor locations. Sixteen events are indicated by the dot symbols and the single large 'bang' event is indicated by '*'. The circles show the mean t_0 of the 16 events.

Figure 5 shows data from the sensors arranged around the base of the rectangular waveguide, where it joins the coupler cell. The lower line in the figure has the slope given by the data from sensors number 6 and 5. In this case, v is about 20% higher than in figure 4, presumably because of the large plate, with the coupling slot, that terminates the waveguide in the vacuum chamber, and effectively reduces the separation between the sensors. The upper line has the opposite sign slope in order to show their intersection point, presumably close to the start point of the wave. The intersection point is about 85

mm from the aisle side edge of the waveguide (about 230 mm x 70 mm). This location is close to the end of the coupling slot inside.

On several occasions we heard a very load bang from within the TTF enclosure, not to be confused with the much smaller acoustic emission signals. For each such case, the RE protection interlock was triggered. One of the 'bang' events is indicated in figure 5 with a somewhat different pattern than the other breakdown events. The bang events sound like they come from the L-band waveguide but they appear to be accompanied with a coupler iris breakdown.

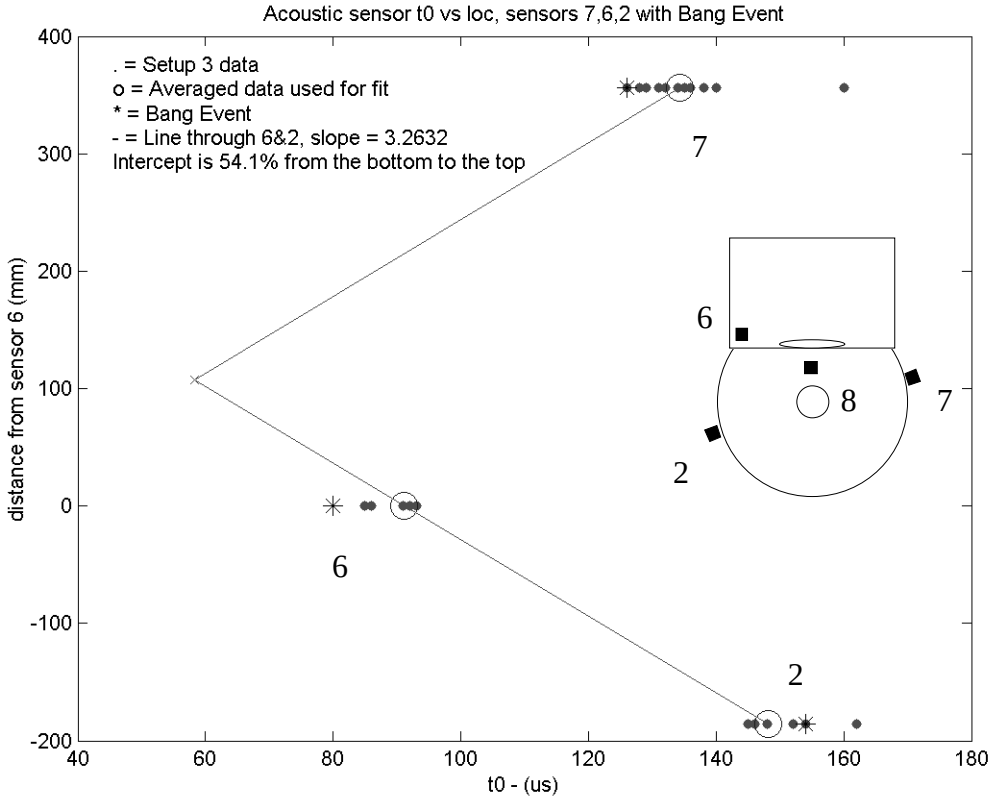

Figure 6: Sensor distance from sensor 6 vs t_0 for the sensors mounted around the circumference of the gun body. The diagram on the right side of the figure indicates the sensor positions in a view looking downstream. As in figure 5, the sixteen events are indicated by the dot symbols and the single large 'bang' event is indicated by '*'. The circles show the mean t_0 of the 16 events.

The relative position of the sensors mounted on the gun body and their response to breakdown events is shown in figure 6. The results are consistent with the above comments, indicating a breakdown location at the top of the cell, towards the aisle side of the gun.

Data from the sensor position configuration 1, in which all sensors were mounted on the aisle side of the gun, is shown in figures 7 and 8.

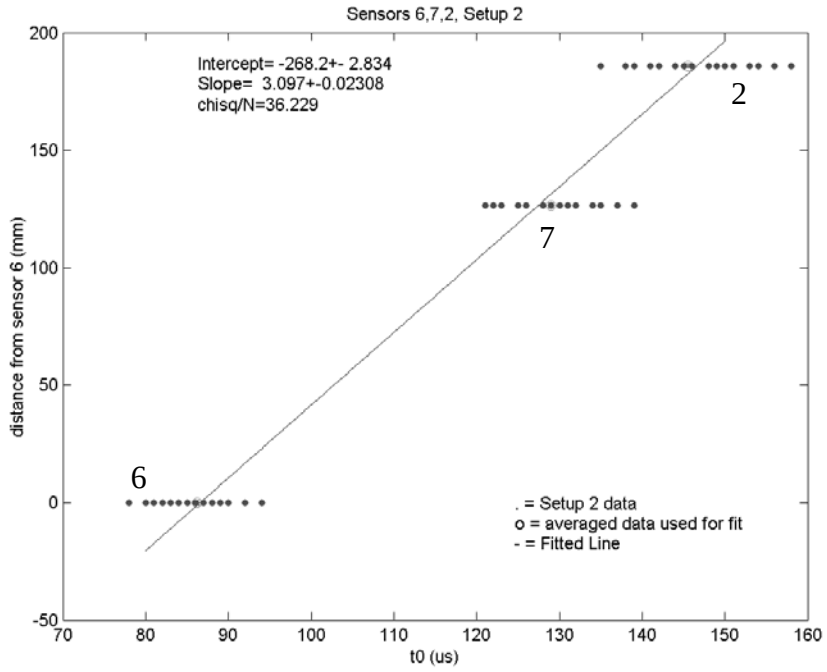

Figure 7: Coupler cavity sensor data for the 24 scope configuration 1 traces, to be compared with figure 5. Sensor 7 is mounted between #2 and #6 in configuration 1.

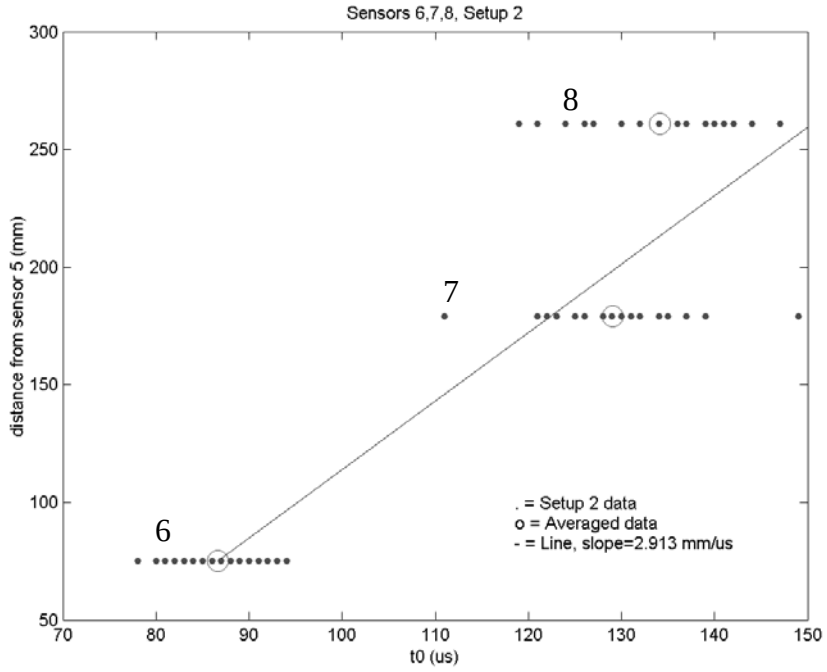

Figure 8: Gun cavity sensor data for configuration 1. This figure is the only one that includes data from sensor 8, mounted close to the cathode. As shown in

figure 3, the signal from sensor 8 has a relatively poorly determined t_0. The line is not a fit but has a slope, v, the same as that in figure 4.

The data in figure 8 do not fall on a line, presumably because the three sensors do not define a simple (axial or radial) section of the cylinder. It was not possible to make a quick measurement of the exact locations of the sensors because of the cathode solenoid.

Conclusions:

We conclude that the RF gun breakdown occurs in the input coupling iris, at a point about 30 mm toward the aisle side of the iris from its center line. With better access to the area, we would be able to locate sensors on each of the wide sides of the L-band waveguide for a more accurate determination.

The acoustic emission sensors give a remarkably accurate indication of the breakdown location in the RF Photocathode gun structure. Almost all of the signals recorded had the same pattern of start times, showing that the observed breakdown events had the same characteristics. As in some NLC X-band structures, it is possible that the highest surface field in the system is in the input coupler iris. Together with small surface defects and breakdown associated damage, that location probably initially was and continues to be susceptible to breakdown. Possible repairs include the use of Scotch-brite to re-polish the surface. Waveguide breakdowns, like those heard from outside the enclosure, may result from the constructive interference between the forward power and the reflected wave caused by a coupler iris breakdown. Possible fixes in this case include the pressurization of the waveguide with SF_6 or the placement of the isolator much closer to the window.

Acknowledgments:

We would like to acknowledge discussions with H. Edwards and E. Colby, who designed and built the gun. We would also like to acknowledge the help of K. Floettmann, K. Rehlich, D. Ramert, S. Schreiber and H. Weise. Their advise and hospitality made this work possible.

References:

[1] M. Gangeluk et.al., "Acoustic Experimental Studies of High Power Modes in Accelerating Structure of Kurchatov SR Source", Proceedings of the 1995 Particle Accelerator Conference.
[2] J. Frisch et.al., "Acoustic Measurements of RF Breakdown in High Gradient RF Structures", Proceedings of the 20th International Linac Conference (SLAC-PUB-8580).
[3] Ian G. Scott, "Basic Acoustic Emission", Gordon and Breach Science Publishers, New York 1991. (for example)
[4] S. Schreiber et.al., "First Experiments with the RF Gun Based Injector for the TESLA Test Facility Linac", Proceedings of the 1999 Particle Accelerator Conference.
[5] http://www.pacndt.com/ and http://www.itc-transducers.com
[6] http://www-project.slac.stanford.edu/lc/8ch_amp_s2.pdf